Nonlinear Model Predictive Control for Improved Water Recovery and Throughput Stability for Tailings Reprocessing

J. J. Burchell[a, b], J. D. le Roux[b], I. K. Craig[b]

[a] *Sibanye-Stillwater, Johannesburg, South Africa*
[b] *Department of Electrical, Electronic and Computer Engineering, University of Pretoria, Pretoria, South Africa.*

Abstract

The reprocessing of tailings aims to recover residual wealth, reclaim or rehabilitate valuable land, or mitigate safety and environmental risks. These aims all support environmental, social, and governance measures that are increasingly placed at the centre of corporate strategy. Tailings reprocessing operations are water intensive, and typically include surge tanks with both level and density averaging objectives to improve the efficiency of downstream water and mineral recovery. In this study, a rigorous dynamic model is derived to describe the rate of change of both the volume and density in these surge tanks. By simulation with industrial data it is demonstrated that the significant input disturbances typical to tailings reprocessing circuits drive a gain inversion in the density model of the surge tank. Since conventional linear averaging control approaches are not ideally suited to deal with gain inversion and multivariable control objectives a nonlinear model predictive controller (NMPC) was derived and implemented on an industrial tailings reprocessing surge tank. Results show a 5 % improvement in water recovery from the plant tailings product, and a 27 % reduction in the standard deviation of the tailings product mass flow.

Keywords: water conservation, dynamic modelling, model predictive control, tailings

1. Introduction

Waste material from mining operations are referred to as mine tailings. The most common method for tailings storage, is behind dammed impoundments commonly referred to as *tailings ponds* or *tailings dams* (Kossoff et al., 2014). The materials used in the construction of tailings dams are often waste rock and the tailings itself with the retaining embankment for the dam constructed at an angle for structural support resulting in the dam taking on a trapezoidal shape. In hard rock mining tailings consists of a fine particle slurry, which when deposited in a tailings dam the solids settles to the bottom and the water is recycled back to operations. To accommodate more waste the height of the dam is increased by extending the crest of the embankment (Martin and McRoberts, 1999).

A tailings dam is reprocessed to recover metals or minerals with sufficient economic value, to reclaim valuable land, or to mitigate safety and environmental risks. Residual high grade value in tailings deposits is a result of inefficiencies in past processing technologies (Falagán et al., 2017). Or, due to a decline in available ore grades, high grade value in tailings deposits is the result of the high grade of the original processed ores (Alcalde et al., 2018). In light of recent catastrophic tailings dam failures (Roche et al., 2017; Santamarina et al., 2019), mining operations are under increased pressure to identify tailings dams at risk and to reprocess them. Moreover, the reprocessing of tailings, specifically in its promotion of land reclamation and as a replacement for processing of virgin ores, and hence a prolonging of primary resource productivity, is consistent with trends towards a circular economy model for mining (Blomsma and Brennan, 2017; Zeng et al., 2021).

The novelty of this paper is that it considers a surge tank control problem not investigated before. The literature on surge tank control mainly considers only flow disturbance rejection and where mass flow is studied constant density is assumed. This paper investigates the surge tank control problem common to hydro-mining based tailings re-processing circuits, where input density disturbances are significant enough to drive model gain inversion. The rigorous dynamic modelling and closed-loop simulations, used to demonstrate model gain inversion and for controller design, and the industrial implementation of a proposed NMPC solution are all novel contributions. There are no published works to compare with the proposed NMPC solution, instead the proposed solution is compared to a baseline industrial control strategy. Both simulated and industrial results demonstrate improved control with the proposed NMPC solution compared to the baseline control strategy.

An NMPC is designed and implemented on a reprocessing circuit that recovers chrome from a platinum group metals (PGM) tailings. This PGM tailings is owned and retreated by Sibanye-Stillwater in the North West province of South Africa.

The NMPC was developed on a section of this circuit tasked with the dewatering of the tailings and with stabil-

ising of its throughput mass flow. The stability of the mass flow positively impacts downstream chrome recovery and hence the profitability of operations, while the dewatering ability of the circuit promotes conservation. Responsible water usage is a key environmental, social, and governance (ESG) measure (Lambooy, 2011) that is growing in importance, as it attracts socially responsible investment (Murad, 2017) under strict auditing criteria.

The development of the NMPC followed the general control problem (GCP) framework for developing model-based controllers (Craig, 1997; Craig and Henning, 2000) outlined in Figure 1. The layout of this paper also follows the GCP framework. In Section 2 the tailings retreatment circuit is studied for control purposes. A rigorous dynamic model is developed and validated in Section 3. Using this model, a control design and analysis is performed in Section 4, motivating for an NMPC control solution. Details for the implemented NMPC are presented in Section 5, and its performance is evaluated in Section 6.

2. Circuit Analysis

Figure 2 presents an overview of the circuit used to recover chrome from the tailings dam. A bulk tailings treatment (BTT) plant dewaters and stabilises the tailings before it is fed to a chrome concentrator plant. This concentrator plant produces chrome using spiral separators to sort the tailings into different chrome grades and a gangue waste product using gravity separation.

To assess the feasibility of this tailings retreatment project, and to motivate for its funding, the following factors were considered:

- The total amount of chrome in the dam estimated from a geological survey.
- Characteristics of the tailings, such as its particle size distribution (PSD), also estimated by a geological survey.
- What recovery[1] would be achieved by the project. The recovery of the project would be influenced by tailings characteristics, such as the PSD, which would affect the efficiency of cyclones and spirals.
- What would be the operating throughput[2], which would largely be influenced by design considerations such as the sizing of pumps, spirals, thickeners, etc.
- The expected chrome price over the life of the project.
- The operating costs over the life of the project.

[1]Here *recovery* refers to the percentage of chrome in the tailings that would be recovered as product, with all unrecovered chrome lost to the gangue waste.

[2]Here *throughput* refers to the rate, in tons per hour, at which tailings would be processed by the circuit.

Using these factors an internal rate of return (IRR), an estimate of the profitability of the project, can be determined. If the IRR for the project exceeds some minimum acceptable rate of return the project is deemed feasible (Bauer and Craig, 2008).

Of the listed factors influencing the IRR for the project, recovery is by far affected the most by improving the control and operation of the circuit post its commissioning. The total amount of chrome in the dam, the tailings characteristics, and chrome price can not be influenced by the circuit, while operating cost and throughput are largely influenced by circuit design. The key performance indicator for the chrome retreatment circuit is therefore its recovery. During the lifetime of the project, operations are continuously under pressure to achieve a target recovery, and any improvements on this recovery is celebrated as a realisation of the upside potential for the project.

Ultimately, the recovery of the circuit depends on the spiral efficiencies of the chrome concentrator. The process variables influencing spiral efficiency include feed density and flow rate (Russell, 2020; Umadevi et al., 2021). A key control objective for the circuit must be to supply the chrome concentrator with consistent feed as highly variable feed characteristics would negatively effect the efficiency of the spiral separators.

2.1. Circuit operation

Figure 3 presents an overview of the tailings dam operations. High pressure water is pumped from the BTT plant, and used to erode the dam into a tailings slurry. The tailings runs through naturally formed channels into a sump. This sump contains a floating barge and a vertical pump.

Two operators oversee key re-mining operations at the tailings dam. The first operator manages the positioning of a high pressure hose that targets the tailings dam face, and tries to cut the face at a steady rate in a first attempt to produce a consistent tailings density. The second operator manages sump operations, agitating the sump with high pressure water to avoid excessive settling of solids in an attempt to improve the consistency of the tailings density to the BTT plant. The density of the tailings to the BTT plant is monitored by the BTT control room. Requests for density adjustment are communicated via hand radio to the tailings dam operators.

The flowsheet for the BTT plant is presented in Figure 4. It uses a large vibrating screen to remove vegitation debris that unavoidably makes its way into the tailings feed. A surge tank is then used to reduce the variability of the tailings density and flow, followed by a hydrocyclone, thickener, and holding tank for dewatering and to further reduce the variability of the tailings feed to the downstream chrome concentrator.

The BTT plant supplies the tailings dam with the water it requires for its operations. Any solids remaining in the thickener overflow is recycled back to the tailings dam

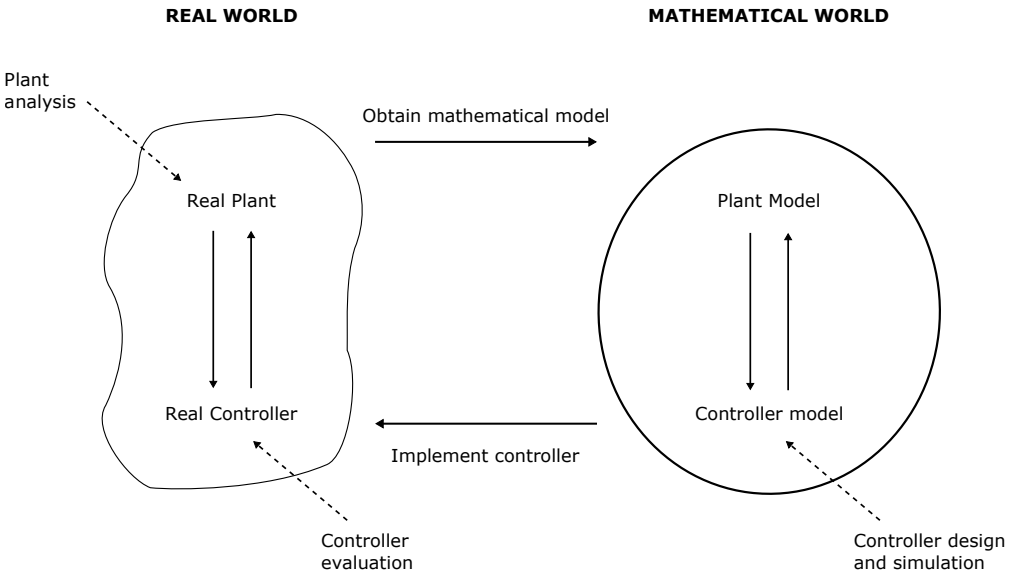

Figure 1: The general control framework for developing advanced control systems.

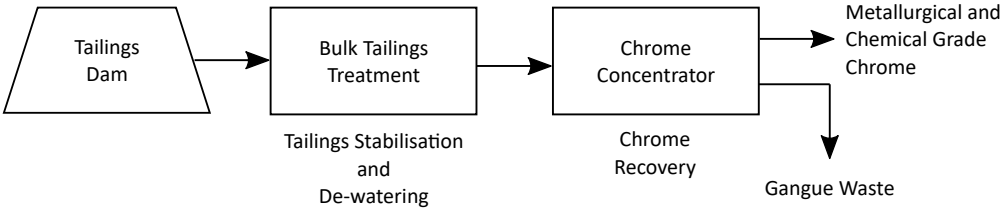

Figure 2: Chrome recovery circuit.

resulting in wasteful rework. Rework is not only wasteful in increasing the per ton processing cost of operations, it also increases water usage as some water is inevitably lost to evaporation. The dewatering ability of the BTT plant refers to its capacity to remove solids from the thickener overflow, which is exclusively influenced by hydrocyclone and thickener efficiencies.

The performance of the plant is measured on its ability to dewater the tailings fed to it and on the variability of the tailings it supplies to the chrome concentrator. Since the feed density to a hydrocyclone and the pressure drop across it both affect hydrocyclone efficiency (Ntengwe and Witika, 2011; Ghodrat et al., 2016), compounding improvements in both hydrocyclone and thickener efficiencies can be achieved by reducing the variability of the surge tank density and output flow. Consequently, the work presented here focused on improving the control of the surge tank in the BTT plant.

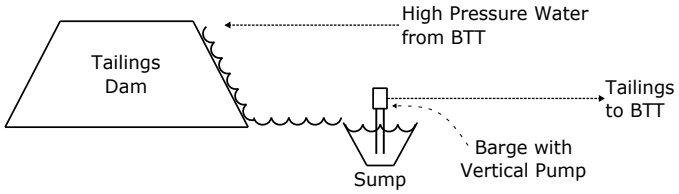

Figure 3: Overview of the Tailings Dam operations.

2.2. Surge tank control approaches

Surge tanks are processing units widely used to avoid the propagation of incoming disturbances to downstream processes. The controller design for surge tanks is a well studied topic with regards to the attenuation of incoming flow disturbances. Flow disturbance rejection in surge tanks is generally described as an *averaging level control* problem.

For averaging level control, the objective is to smooth the outlet flow while ensuring the tank level is constrained within a specified range. This control problem was studied as a proportional-integral-derivative (PID) tuning problem (Reyes-Lúa et al., 2018; Luyben, 2020), an optimal control problem (Lee and Shin, 2009), a nonlinear control problem (Sanchis et al., 2011), and a robust MPC problem (Rosander et al., 2012). In Sparbaro and Ortega (2007) the level averaging control problem is addressed using a mass balance approach. Crisafulli and Peirce (1999) apply a gain scheduled feedforward controller on a surge tank in a raw cane sugar factory to attenuate flow disturbances and improve clarification of cane juice. Although the literature on averaging level control mainly considers single surge tank processes, some investigated control approaches apply to multiple tank processes (Khan and Spurgeon, 2006;

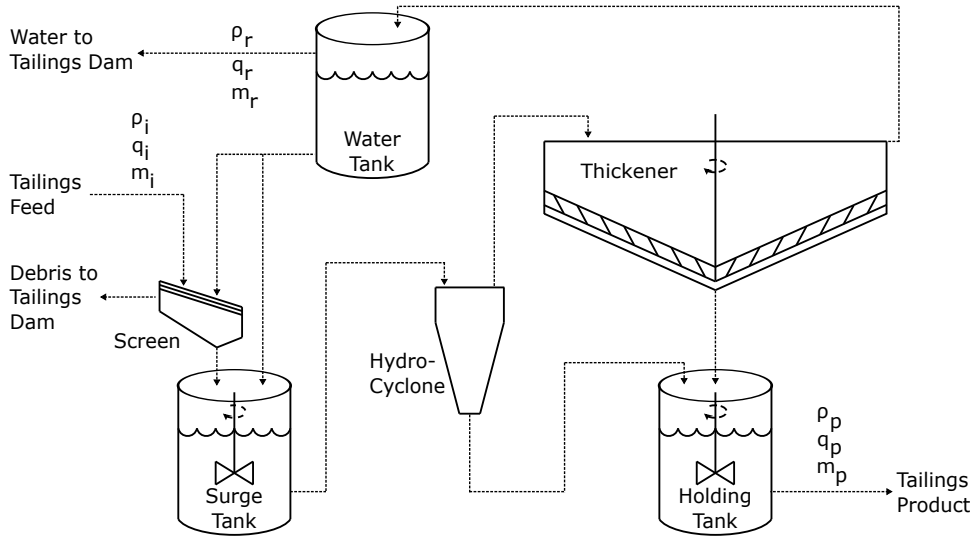

Figure 4: Flowsheet of the BTT plant.

Table 1: A description of key surge tank and holding tank process variables.

Surge Tank Variables	Units	Description
q_i	m^3/h	Feed rate from tailings dam
ρ_i	t/m^3	Density from tailings dam
m_i	t/h	Mass flow from tailings dam
ρ	t/m^3	Density in surge tank
v	m^3	Volume in surge tank
l	%	Surge tank level
q_w	m^3/h	Surge tank water addition rate
q_o	m^3/h	Feed rate from surge tank
ρ_o	t/m^3	Density from surge tank
Holding Tank Variables	**Units**	**Description**
q_p	m^3/h	Plant output flow
ρ_p	t/m^3	Plant output density
m_p	t/h	Plant output mass flow
Water Tank Variables	**Units**	**Description**
q_r	m^3/h	Flow to tailings dam
ρ_r	t/m^3	Density to tailings dam
m_r	t/h	Mass flow to tailings dam

Sbarbaro and Ortega, 2007).

The surge tank control problem addressed herein deviates from the literature in that it considers not only level averaging control, but also the stabilisation of an incoming tailings feed. Here stabilisation refers to reducing the variability in flow, density, or mass flow of the tailings. The averaging level control literature reviewed exclusively adjusted only the output flow from the surge tank, or multiple surge tank systems, to dampen incoming flow disturbances. The design of the surge tank in the BTT flowsheet deviates from these reviewed surge tank systems, as it includes a line for controlled water addition. This water addition line thus allows for an extra degree of freedom to address the tailings stabilisation objective. Moreover, the literature reviewed generally assumed a constant input density while the control solution presented here addresses significant input density fluctuations that result in a model gain inversion.

2.3. Baseline surge control strategy for the BTT surge tank

An example of plant input dynamics and the baseline surge control strategy is presented in the 10-hour long dataset shown in Figure 5. This dataset was recorded while the plant was under normal operation, i.e. while the plant was not under start-up or shut-down conditions.

The input density varies at times rapidly and generally over a large range. This is expected due to the highly manual operation of the process at the tailing dam, as described in Section 2.

The input flow is seemingly inversely proportional to the input density. This is expected as the baseline control strategy did not manipulate the input flow directly but maintained a fixed pump speed. Consequently, flow dynamics are dominated by density fluctuations.

The baseline control strategy clearly implements steps in water addition and output flow rate to maintain tank level and tank density within acceptable ranges. On further investigation, the output flow rate is not directly adjusted to maintain the tank level. There is a pressure controller on the output line to keep the pressure across the hydro-cyclone constant. The set-point to this pressure controller is stepped to affect a change in output flow so as to maintain the tank level within a range.

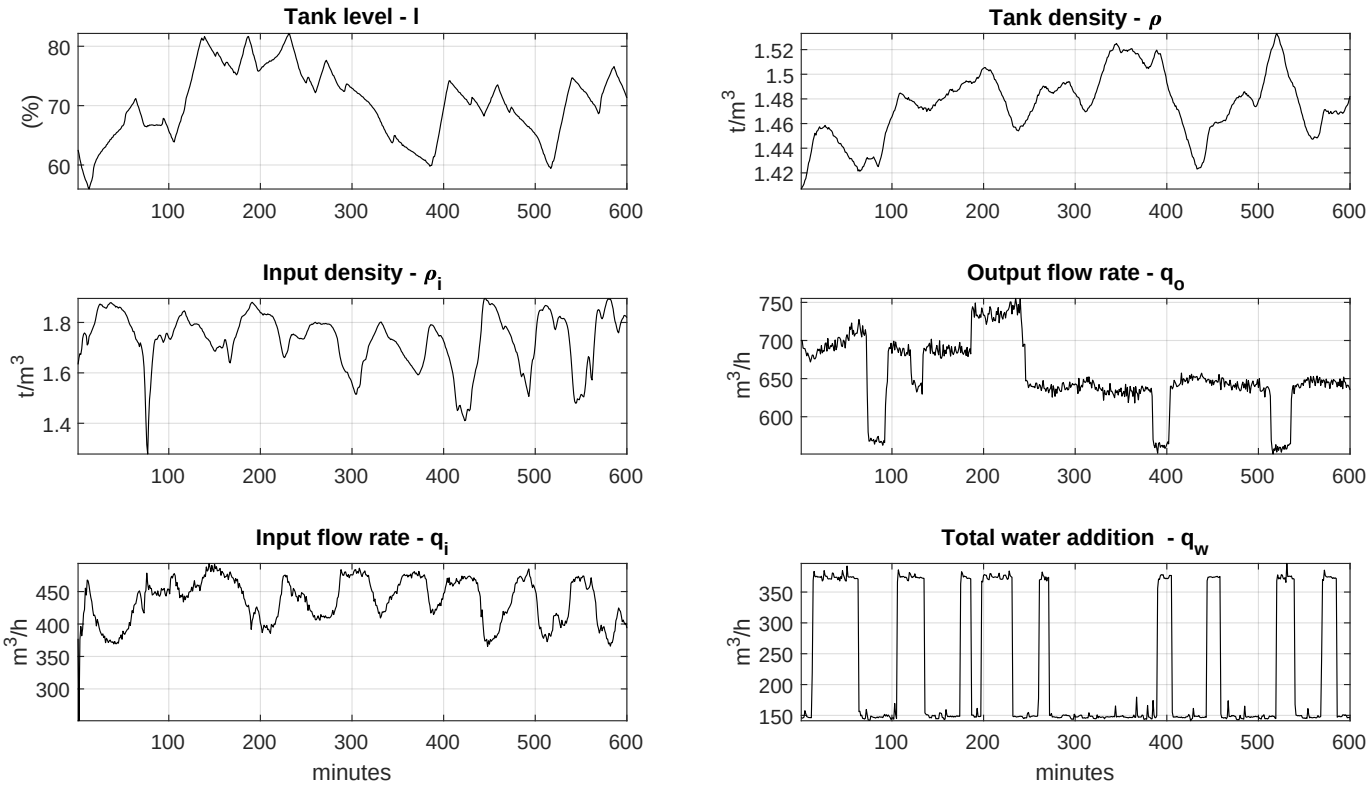

Figure 5: Dataset obtained from the BTT surge tank while operated under the baseline surge control strategy.

3. Dynamic Modelling

3.1. Nonlinear state-space model

A nonlinear model of the surge tank was developed to assess how effective different control strategies are at rejecting the typical input density and flow disturbances from the tailing dam. Figure 6 presents a simplified schematic diagram of the surge tank with all relevant process variables labelled. The nomenclature for the key surge and holding tank variables is shown in Table 1. The input flow rate, water flow rate, and output flow rate are respectively q_i, q_w, and q_o. The tank volume, derived from a tank level measurement, is v, and the input density, the density in the tank, and the output density are respectively ρ_i, ρ, and ρ_o.

Assuming perfect mixing, i.e. $\rho = \rho_o$, and conservation of mass the rate of accumulation of mass in the surge tank is:

$$\frac{d\rho v}{dt} = \rho_i q_i + q_w - \rho q_o. \tag{1}$$

The differential term on the left is expanded using the chain rule:

$$v\frac{d\rho}{dt} + \rho\frac{dv}{dt} = \rho_i q_i + q_w - \rho q_o. \tag{2}$$

Assuming no volume change during mixing, which is a reasonable assumption when modelling slurry dynamics

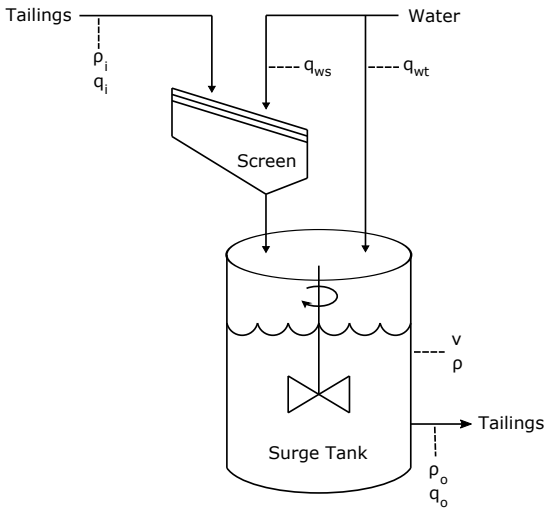

Figure 6: BTT surge tank.

(Dontsov and Perice, 2014), the volume in the surge tank will be conserved and the rate of change of volume in the surge tank can be expressed as:

$$\frac{dv}{dt} = q_i + q_w - q_o. \tag{3}$$

Substituting (3) into (2) gives the rate of accumulation

of density independent of the rate of change in volume:

$$\frac{d\rho}{dt} = \frac{q_i\rho_i - \rho(q_i + q_w) + q_w}{v}. \tag{4}$$

The nonlinear model of the surge tank follows from (3) and (4):

$$\begin{bmatrix}\dot{v}\\ \dot{\rho}\end{bmatrix} = \begin{bmatrix} q_i + q_w - q_o \\ \frac{1}{v}(q_i\rho_i - \rho(q_i + q_w) + q_w)\end{bmatrix}. \tag{5}$$

In subsequent sections, the following functional form of the nonlinear model in (5) is used:

$$\begin{aligned}\dot{\mathbf{x}} &= \mathbf{f}(\mathbf{x}, \mathbf{u}, \mathbf{d}),\\ \mathbf{y} &= \mathbf{h}(\mathbf{x}).\end{aligned} \tag{6}$$

The elements of the state vector is $\mathbf{x} = \begin{bmatrix} v & \rho \end{bmatrix}^\top$, the input is $\mathbf{u} = \begin{bmatrix} q_i & q_w \end{bmatrix}^\top$, and the disturbance vector is $\mathbf{d} = \begin{bmatrix} \rho_i & q_o \end{bmatrix}^\top$. Since the tank volume is not directly measured, an output vector $\mathbf{y}$ is specified that defines a mapping between the measurable outputs, tank level l and tank density ρ, and $\mathbf{x}$:

$$\mathbf{y} = \begin{bmatrix} l \\ \rho \end{bmatrix} = \begin{bmatrix} \frac{100}{v_t} & 0 \\ 0 & 1 \end{bmatrix} \mathbf{x}, \tag{7}$$

with v_t the total volume of the surge tank.

3.2. Model validation

The model in (5) is validated using the dataset presented in Figure 5. The tank level and tank density was initialised with the tank volume and density measured at $t = 0$, and the simulated outputs $\mathbf{y}_{sim}$ was obtained by subjecting the model to the measured inputs $\mathbf{u}$ and disturbances $\mathbf{d}$. The simulated and measured tank density and level is shown in Figure 7. Table 2 presents a summary of the model validation results, comparing the difference between simulated and measured tank level and density using the mean absolute error (MAE) and coefficient of determination (R^2).

Table 2: Model validation results, comparing differences between the simulated and measured tank level and density using the mean absolute error (MAE) and coefficient of determination (R^2).

Variable	MAE	R^2
l	2.237 %	0.796
ρ	0.009 t/m^3	0.837

The model validation results show good correspondence between the measured and simulated values. An R^2 of 0.796 for the tank level suggests that approximately 80 % of the variance is explained by the simulated level, while an MAE of 2.237 % represents a small deviation between the measured and simulated tank levels. Similarly, with an R^2 of 0.837 and an MAE of 0.009 t/m^2 there is good correspondence between the simulated and measured tank density. Small deviations in the model accuracy may be due to inaccuracies in the measurements, e.g. imperfect instrumentation calibration, while deviation between specifically the simulated and measured tank density may be due to imperfect mixing.

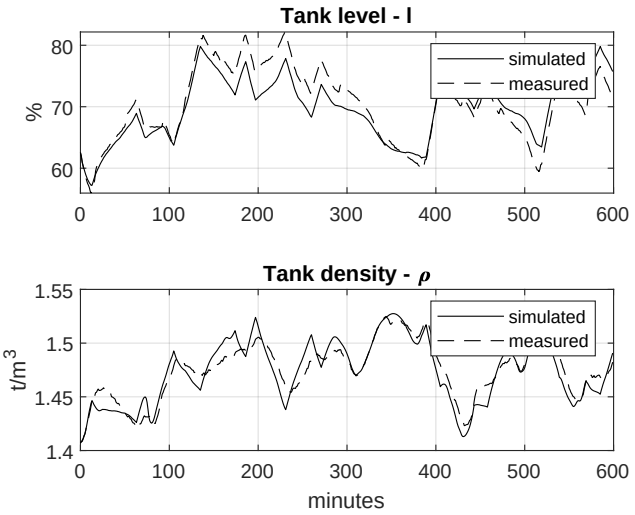

Figure 7: Validation of the nonlinear model.

3.3. Linear approximation

A linear approximation of a system is generally useful as it allows the application of the well developed theory on linear systems to explore the dynamic behaviour of a system (Skogestad and Postlethwaite, 2005). An in-depth exploration of the dynamic behaviour of this surge tank is not presented here, however, the interested reader is referred to Rokebrand et al. (2020, 2021). A linear approximation for the surge tank model in (6) is described here and used in Section 4 to motivate for the use of an NMPC solution.

With the expression for the accumulation of volume in (3) already linear, a linear approximation of the surge tank requires only the Taylor series expansion of (4). Taking the functional form:

$$\frac{d\rho}{dt} = f_\rho(q_i, q_w, q_o, \rho_i, \rho, v), \tag{8}$$

and applying a multivariate Taylor series expansion about the nominal steady-state operating point $\bar{x} = [\bar{q}_i, \bar{q}_w, \bar{\rho}_i, \bar{\rho}, \bar{v}]^\top$, and ignoring the higher order terms gives:

$$f_\rho(q_i,q_w,q_o,\rho_i,\rho,v) \cong f_\rho(\bar{x}) + \left.\frac{\partial f_\rho}{\partial q_i}\right|_{\bar{x}} \delta q_i + \left.\frac{\partial f_\rho}{\partial q_w}\right|_{\bar{x}} \delta q_w + \left.\frac{\partial f_\rho}{\partial q_o}\right|_{\bar{x}} \delta q_o + \left.\frac{\partial f_\rho}{\partial \rho_i}\right|_{\bar{x}} \delta \rho_i + \left.\frac{\partial f_\rho}{\partial \rho}\right|_{\bar{x}} \delta \rho + \left.\frac{\partial f_\rho}{\partial v}\right|_{\bar{x}} \delta v$$

$$\cong f_\rho(\bar{x}) + \frac{\bar{\rho}_i - \bar{\rho}}{\bar{v}}\delta q_i + \frac{1-\bar{\rho}}{\bar{v}}\delta q_w + \frac{\bar{q}_i}{\bar{v}}\delta\rho_i - \frac{\bar{q}_i + \bar{q}_w}{\bar{v}}\delta\rho - \frac{\bar{q}_i\bar{\rho}_i + \bar{q}_w - (\bar{q}_i+\bar{q}_w)\bar{\rho}}{\bar{v}^2}\delta v. \tag{9}$$

By definition, at steady-state $\bar{q}_i + \bar{q}_w - \bar{q}_o = 0$ and $\bar{q}_i\bar{\rho}_i + \bar{q}_w - \bar{q}_o\bar{\rho} = 0$ such that (9) reduces to:

$$f_\rho(q_i,q_w,q_o,\rho_i,\rho,v) \cong f_\rho(\bar{x}) + \frac{\bar{\rho}_i - \bar{\rho}}{\bar{v}}\delta q_i + \frac{1-\bar{\rho}}{\bar{v}}\delta q_w + \frac{\bar{q}_i}{\bar{v}}\delta\rho_i - \frac{\bar{q}_o}{\bar{v}}\delta\rho. \tag{10}$$

The continuous state-space representation of a linear system with N_x states, N_u manipulated inputs, N_d disturbance inputs, and N_y outputs is:

$$\frac{d\mathbf{x}(t)}{dt} = \mathbf{A}\mathbf{x}(t) + \mathbf{B}\mathbf{u}(t) + \mathbf{C}\mathbf{d}(t)$$
$$\mathbf{y}(t) = \mathbf{D}\mathbf{x}(t), \tag{11}$$

where $\mathbf{x}(k) \in \mathbb{R}^{N_x\times 1}$ is the state vector, $\mathbf{u}(k) \in \mathbb{R}^{N_u\times 1}$ is the input vector, $\mathbf{d}(k) \in \mathbb{R}^{N_d\times 1}$ is the disturbance vector, $\mathbf{y}(k) \in \mathbb{R}^{N_y\times 1}$ is the output vector, $\mathbf{A} \in \mathbb{R}^{N_x\times N_x}$ is the state matrix, $\mathbf{B} \in \mathbb{R}^{N_u\times N_u}$ is the input matrix, $\mathbf{C} \in \mathbb{R}^{N_d\times N_d}$ is the disturbance matrix, and $\mathbf{D} \in \mathbb{R}^{N_y\times N_y}$ is the output matrix.

The linear model of the surge tank follows from (3), (7), and (10):

$$N_x = N_y = 2, N_d = N_u = 2,$$
$$\mathbf{A} = \begin{bmatrix} 0 & 0 \\ 0 & -\frac{\bar{q}_o}{\bar{v}} \end{bmatrix}, \mathbf{B} = \begin{bmatrix} 1 & 1 \\ \frac{\bar{\rho}_i - \bar{\rho}}{\bar{v}} & \frac{1-\bar{\rho}}{\bar{v}} \end{bmatrix},$$
$$\mathbf{C} = \begin{bmatrix} -1 & 0 \\ 0 & \frac{\bar{q}_o}{\bar{v}} \end{bmatrix}, \text{ and } \mathbf{D} = \begin{bmatrix} \frac{100}{v_t} & 0 \\ 0 & 1 \end{bmatrix}. \tag{12}$$

4. Controller Design and Simulation

4.1. Model predictive control

Model predictive control (MPC) refers to a class of advanced control algorithms that have been shown to be effective in the process industry in dealing with multivariable constrained control problems (Qin and Badgwell, 2003; Meyer et al., 2019). MPC relies on a model to predict the state and output responses of a system over a finite prediction horison N_p.

At each sampling interval k the MPC solves for a set of control moves over a control horison N_c by minimising an objective function $J(.)$, given estimates of the initial state of the system $\mathbf{x}(k)$, measurements of the initial system manipulated inputs $\mathbf{u}(k)$, disturbance inputs $\mathbf{d}(k)$, outputs $\mathbf{y}(k)$, and a desired reference trajectory for the system output $\mathbf{y}_{ref}$. The measured disturbance inputs are assumed to remain constant over the prediction horison N_p. This constrained optimisation problem can be expressed as follows:

$$\min_{\mathbf{u}(k+1|k),\ldots,\mathbf{u}(N_c+1|k)} \quad J\left(\mathbf{u}, \mathbf{d}(k), \mathbf{x}(k), \mathbf{y}_{ref}\right)$$

subject to:

$$\begin{aligned}
&\mathbf{x} \in \mathbb{R}^{N_x\times N_p}, \quad \mathbf{x}_l \le \mathbf{x} \le \mathbf{x}_h;\\
&\mathbf{u} \in \mathbb{R}^{N_u\times N_c}, \quad \mathbf{u}_l \le \mathbf{u} \le \mathbf{u}_h;\\
&\mathbf{y} \in \mathbb{R}^{N_y\times N_p}, \quad \mathbf{y}_l \le \mathbf{y} \le \mathbf{y}_h;\\
&\mathbf{x}(k+i+1|k) = \mathbf{f}_k(\mathbf{x}(k+i|k), \mathbf{u}(k+i|k), \mathbf{d}(k)),\\
&\mathbf{y}(k+i|k) = \mathbf{h}_k(\mathbf{x}(k+i|k)),\\
&\qquad\qquad \forall\ i = 1, 2, ..., N_c;\\
&\mathbf{x}(k+j+1|k) = \mathbf{f}_k(\mathbf{x}(k+j|k), \mathbf{u}(k+N_c|k), \mathbf{d}(k)),\\
&\mathbf{y}(k+j|k) = \mathbf{h}_k(\mathbf{x}(k+j|k)),\\
&\qquad\qquad \forall\ j = N_c+1, N_c+2, ..., N_p.
\end{aligned} \tag{13}$$

The system state $\mathbf{x}$ is constrained to operate within upper and lower bounds, $\mathbf{x}_h$ and $\mathbf{x}_l$ respectively, as are the system inputs and outputs, $\mathbf{u}$ and $\mathbf{y}$. Note that the optimisation procedure solves for only N_c control vectors, with the input vector kept constant at $\mathbf{u}(k+N_c)$ for the remainder of time intervals in the prediction horison N_p.

The cost function in (13) is defined as:

$$J(\mathbf{u}, \mathbf{d}(k), \mathbf{x}(k), \mathbf{y}_{ref}(k)) = \sum_{i=1}^{N_p} \|\mathbf{y}_{ref}(k+i) - \mathbf{y}(k+i|k)\|^2_{\mathbf{Q}} + \sum_{i=1}^{N_c} \|\Delta\mathbf{u}(k+i|k)\|^2_{\mathbf{S}} \tag{14}$$

with $\mathbf{y}_{ref} \in \mathbb{R}^{N_y\times N_p}$ and $\Delta\mathbf{u}(k+i|k) = \mathbf{u}(k+i|k) - \mathbf{u}(k+i-1|k)$.

Here $\mathbf{Q}$ and $\mathbf{S}$ are diagonal matrices used to weight the relative importance of the controlled and manipulated variables respectively.

At each sampling instant k the MPC solves for N_c control vectors and implements the first control move $\mathbf{u}(k+1)$. At the following instant new measurements are obtained from the system and the optimisation procedure is repeated.

4.2. Linear vs nonlinear MPC

The linear model in (12) was derived on the assumption that higher order terms in the Taylor series expansion can be disregarded, since close to the nominal operating point $\bar{x}$ higher order terms will be approximately zero. Processes, of course, continuously deviate from their nominal operating points and plant-model mismatch in the form of inaccuracies between the true system dynamics and the linear model predictions can not be avoided (Olivier and Craig, 2015).

Considering that the vast majority of industrial model predictive control solutions rely on linear models to control nonlinear processes (Qin and Badgwell, 2003), plant-model mismatch is often disregarded. This can be explained by noting that it is comparatively cheap to develop linear models, typically by assuming that the dynamic responses of the system follow first-order-plus-time delay (FOPTD) transients, and by fitting FOPTD models to data obtained from step testing. Compared to a first principles approach to obtain a nonlinear process model, a linear model obtained from step tests is markedly less complicated and time consuming.

Generally, linear approximations are at least accurate to the direction of relationships between model inputs and outputs. This is often considered *good enough* for control since the system can be driven towards a desired operating point. Moreover, feedback control has a linearising effect as it keeps the plant close to an operating point (Skogestad and Postlethwaite, 2005). Ultimately, the negative effects of some model mismatch is likely never considered when a linear MPC achieves noteworthy improvements compared to a baseline control system.

A linear approximation for this surge tank model would not be sufficient, however, since the observed deviation of input density from the tailings dam would cause inversion of the direction of the relationship between input flow q_i and tank density ρ. For the linear approximation of the surge tank model the term in the input matrix $\mathbf{B}$ in (11) associated with the input flow q_i will always be positive. The constant flow of water q_w to maintain the screen dilutes the incoming tailings, and guarantees that:

$$\frac{\bar{\rho}_i - \bar{\rho}}{\bar{v}} > 0. \tag{15}$$

A linear MPC relying on the model in (11) would therefore always use q_i to increase ρ. However, the re-mining process followed at the tailings dam, described in Section 2, relies on manual operations and is exposed to various environmental factors that results in an input density ρ_i that varies over a large range. This high degree of variation often results in a scenario where the direction of the relationship between q_i and ρ would be negative, i.e. an inversely proportional relationship where an increase in q_i would result in a decrease in ρ.

This *gain inversion* is demonstrated in Figure 8 for a fictitious, although reasonably likely, steady-state operating point. The steady-state operating point considered is:

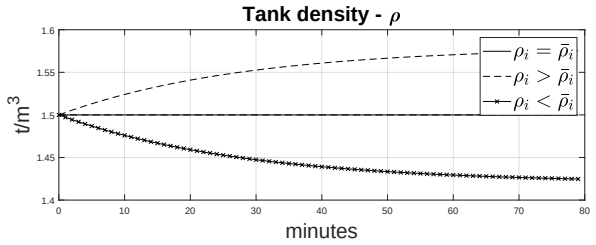

Figure 8: Gain inversion in the relationship between input flow q_i and tank density ρ as a result of significant variance in the instantaneous input density ρ_i.

$\bar{q}_i = 600$ m^3/h, $\bar{q}_w = 150$ m^3/h, $\bar{q}_o = 750$ m^3/h,

$\bar{\rho}_i = 1.625$ t/m^3, $\bar{\rho} = 1.5$ t/m^3, and

$v = 350$ m^3/h.

Figure 8 simulates three scenarios using the nonlinear model in (5). For all three the instantaneous input flow q_i remains constant and equal to the steady-state input flow $\bar{q}_i$. In the first scenario $(-)$, representing the case with no model mismatch, the instantaneous input density ρ_i remains constant and equal to the steady-state input density $\bar{\rho}_i$. In the second scenario $(--)$ $\rho_i = \bar{\rho}_i + 0.1$. In the third scenario $(-\times)$, $\rho_i = \bar{\rho}_i - 0.1$.

Therefore, for the particular scenario where a controller is tasked to maintain ρ at a target density ρ_{target}, with $\rho_i < \bar{\rho}_i$ and $\rho < \rho_{target}$, a linear model based controller would increase q_i, further driving ρ away from ρ_{target}. It is therefore important to account for the demonstrated gain inversion in the controller design. Therefore, an NMPC is chosen based on the nonlinear model in (6).

The main drawback of NMPC is the computational burden, and associated time delay in solving its non-convex optimisation problem. Generally speaking this is not much of a concern in the process industry, where the dynamics of systems are relatively slow allowing for more computationally intensive control approaches (Gros et al., 2020). For nonlinear systems with faster dynamics, where the range of operation requires nonlinearity to be accounted for, adaptive MPC (Adetola et al., 2009) and gain scheduled MPC (Ilka and Veseleý, 2015; Wiid et al., 2021) can be used.

4.3. Controller simulations

The aim is to maintain the surge tank density at a target density ρ_{target}. This target density is likely to change slowly over time due to changes in the nominal input density ρ_i, which in turn is due to slow changes in equipment condition and tailings characteristics. A strategy for operations can be to set ρ_{target} to the nominal tank density $\bar{\rho}$ achieved during the previous day. Note, the nominal output flow $\bar{q}_o$ and tank density $\bar{\rho}$ sets the throughput of the chrome recovery circuit as a whole. Hence, operations need to maintain ρ_{target} within an acceptable range to deliver on the assumptions that motivated the business case discussed in Section 2.

Two controller simulations were performed. In the first simulation the surge tank level was allowed to move freely within upper and lower limits of 90 % and 40 % respectively. In practice a lower limit is chosen to protect the agitator assembly, which would get damaged if it was allowed to operate under no load. An upper limit is chosen to avoid overflow should there be inaccuracies in the level measurement and/or an unmeasured input into the tank. By allowing the tank level to move freely within these limits, the NMPC can absorb short term disturbances in for example input density ρ_i by reducing the input flow q_i.

Because of the settling of solids in the tailings dam sump ρ_i can decrease significantly. The tailings dam operators implement measures to alleviate these settling issues, but for the duration of the low input density the controller could decrease the input flow q_i to dampen the impact on ρ.

In the second simulation the surge tank level was maintained at a set point of 90 %. Note that in (4), the expression for the rate of accumulation of density, the volume appears in the denominator. Therefore, the tank volume acts as a buffer and maintaining the surge tank at a high volume will provide improved disturbance rejection.

A summary of the process variable targets and constraints used in the simulations is presented in Table 3. Apart for the level all targets and constraints were identical in both simulations.

Table 3: A summary of the process variable targets and constraints used in the controller simulations.

Process Variable	Target or Range Constraint
Level in simulation 1 l_1	$40 \leq l_a \leq 90$ %
Level in simulation 2 l_2	90 %
Tank density ρ_{target}	1.475 t/m^3
Input flow q_i	$250 \leq q_i \leq 500$ m^3/h
Total water addition q_w	$100 \leq q_w \leq 400$ m^3/h
Input flow step size Δq_i	$\Delta q_i \leq 150$ m^3/h
Water step size Δq_w	$\Delta q_w \leq 50$ m^3/h

The input flow is constrained to operate within upper and lower limits of 250 m^3/h and 500 m^3/h respectively. Plant knowledge dictates that the minimum input flow must be 250 m^3/h to avoid solids settling in the input line, which can result in the line choking. The maximum input flow is set to the maximum observed flow in the dataset used for model validation, as presented in Figure 5.

The input water is constrained to operate within upper and lower limits of 100 m^3/h and 400 m^3/h respectively. The minimum flow of water to the surge tank is set as the flow required to operate the screen. The maximum water addition is set as the maximum flow observed in the validation dataset.

A small cost is assigned to avoid overly aggressive moves in the input variables in order to minimise equipment wear. By simulation on the validation dataset it can be shown that setting both diagonal elements in S to 5×10^{-6} ensures that $\Delta q_i \leq 150$ m^3/h and $\Delta q_w \leq 50$ m^3/h.

The design of the NMPC can be summarised as the constrained optimisation problem in (13) and (14) with:

$$N_p = 20, \;\; N_C = 10, \;\; \mathbf{y}_{ref} = \rho_{target},$$
$$\mathbf{Q} = 1, \text{ and } \mathbf{S} = \begin{bmatrix} 5 \times 10^{-6} & 0 \\ 0 & 5 \times 10^{-6} \end{bmatrix}. \qquad (16)$$

The model is descretised using the 4$^{\text{th}}$ order Runge-Kutta method, with a step size of 1 minute. The simulated model outputs are initialised to the measured initial conditions of the system. Figure 9 presents a block diagram of the NMPC and the plant model configuration used to obtain the simulated results.

Figure 10 and Figure 11 present the results for simulations 1 and 2 respectively. In both simulations the plant model was subjected to the measured input flow and output flow disturbances shown in Figure 5.

In both simulations the NMPC maintains the tank level within the specified level range or at set point. The NMPC is able to reject much of the input density disturbances, however, it is unable to maintain the tank density ρ at the target density ρ_{target} at very low input densities.

Figure 12 compares the tank density ρ *measured*, obtained from the plant under baseline control, to the simulated tank densities, ρ *simulated 1* and ρ *simulated 2*, under NMPC control. The simulated NMPC performance improves on the baseline performance in both simulations. The standard deviation of the surge tank density in simulation 1 was 54 % lower compared to the measured density, while the standard deviation of the surge tank density for simulation 2 was 33 % lower. Therefore, by simulation it is shown that an NMPC control strategy that maintains the tank level within a specified range is the superior control strategy.

5. Controller Implementation

The NMPC simulated in the previous section was implemented on the industrial plant using the GEKKO optimisation and machine learning library (Beal et al., 2018) in Python. Other than the simulation study, the objective for the NMPC implemented on the plant was to maintain the surge tank level within 70 % and 90 %, with a target density of 1.45 t/m^3. The level range was chosen, expecting that the pressure controller on the output of the tank adjusts the pressure set point to maintain the tank level within this range. Therefore, to avoid pressure setpoint changes that would negatively effect cyclone efficiency, the same level range as used during simulation was chosen for the NMPC implemented on the plant. The target density was chosen as the nominal output density at the time.

Consider that for the steady-state operating point presented in Section 4.2, $\|\mathbf{B}\| \times \left\|\mathbf{B^{-1}}\right\| = 960 >> 1$. Hence at this operating point the system is ill-conditioned, which

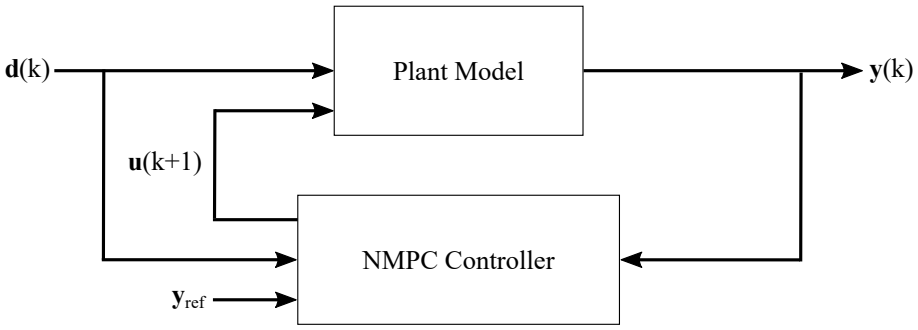

Figure 9: Block diagram of the NMPC controller and plant model configuration used to obtain the simulated results.

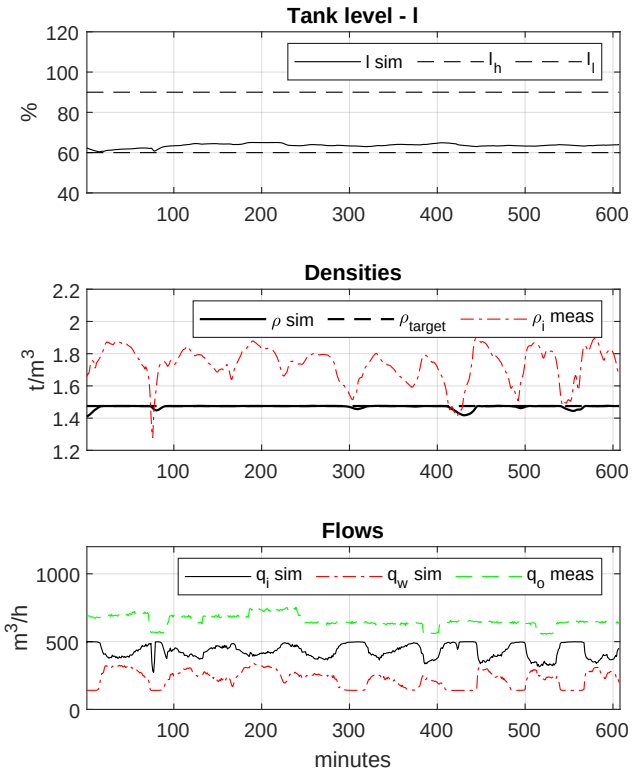

Figure 10: Simulated NMPC control of the surge tank under measured input density and output flow disturbances, with the tank level allowed to travel within a specified range.

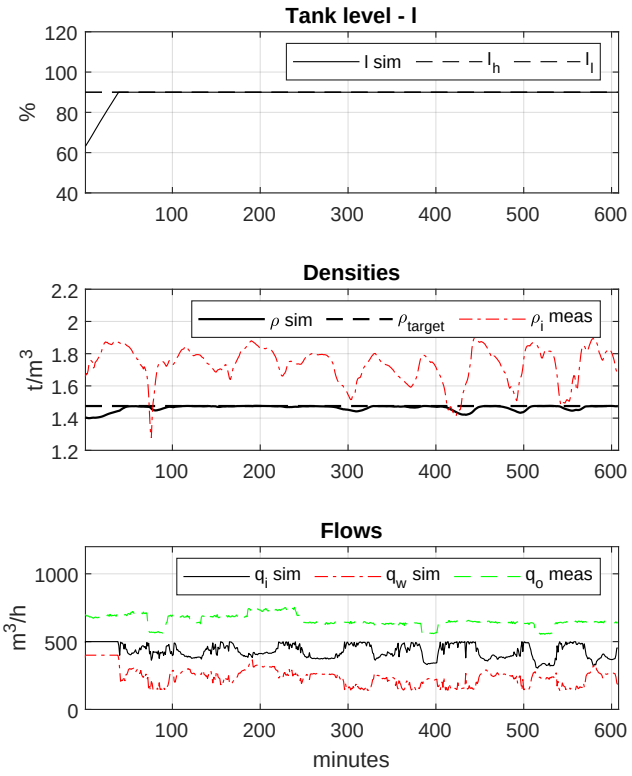

Figure 11: Simulated NMPC control of the surge tank under measured input density and output flow disturbances, with the tank level maintained at set point.

may result in excessively large adjustments in the manipulated inputs **u**. To prioritise equipment health, the NMPC was constrained to not move the input flow to the surge tank by more than 20 m^3/min and the water addition to the surge tank by more than 50 m^3/min.

Custom modules were developed on an Allen-Bradley programmable logic controller (PLC) and a user interface on Wonderware's supervisory control and data acquisition (SCADA) system. These modules allowed, for example, switching between the baseline controller and the NMPC, and monitored communication health using a watchdog timer. A number of interlocks were also implemented on the PLC to disable the NMPC when conditions were not suitable. A key interlock was developed for when the input line would choke. If the surge tank was to remain under NMPC control with an input line choke, the tank density would plummet as the NMPC would demand an ever higher input flow of tailings to counter a dropping density while only water was being added.

6. Results

Figure 13 presents a time series plot of 180-hours before and 60-hours after the NMPC was switched on. This dataset records the hourly-averages of the key surge tank

Table 4: A summary of the results, comparing the differences in mean and standard deviation before and after the NMPC was put online.

Process Variable	Mean Before, After	Accept or Reject h_0 : Equal Mean (Significance)
ρ_i	1.548, 1.560	accept (0.266)
ρ_p	1.478, 1.500	reject (0.002)
q_i	511.186, 524.903	accept (0.164)
q_p	674.531, 674.277	reject (0.022)
m_i	385.274, 423.058	reject (0.000)
m_p	454.584, 472.779	reject (0.001)
Process Variable	Standard Deviation Before, After	Accept or Reject h_0 : Equal Standard Deviation (Significance)
ρ_i	0.147, 0.145	accept (0.476)
ρ_p	0.058, 0.106	accept (0.117)
q_i	89.762, 94.094	accept (0.453)
q_p	16.833, 6.526	accept (0.284)
m_i	52.472, 56.061	accept (0.310)
m_p	42.146, 30.580	reject (0.015)

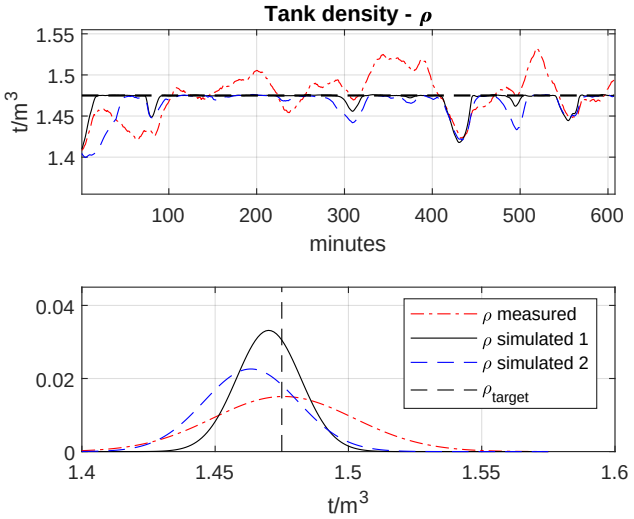

Figure 12: A comparison between the measured tank density under baseline control and the simulated tank density under NMPC control. In simulation 1 the tank level was allowed to travel within a specified range, while in simulation 2 the tank level was maintained at set point.

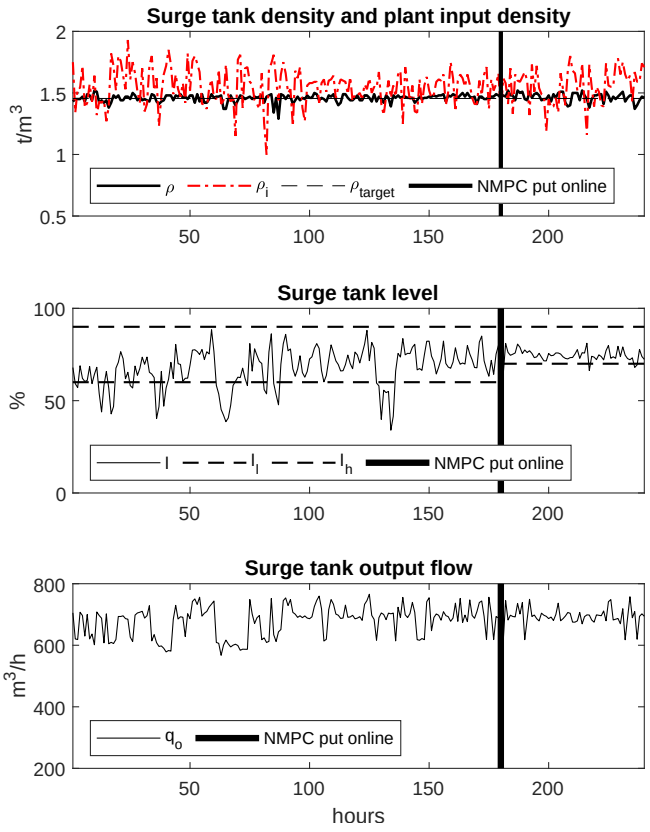

Figure 13: Time series of surge tank variables before and after the NMPC was put online.

measures. The baseline controller maintained the level between 60 % and 90 % by stepping the pressure target on the output line at fixed step sizes. Note, the pressure of the output line is maintained by adjusting the output flow rate q_o. The baseline controller maintained the surge tank density by adjusting the water addition to the tank.

The level under NMPC control has a lower variability, i.e. a lower standard deviation. Although the output flow has lower variability under NMPC control, there remains some variability. Noting that the output flow from the surge tank is adjusted by a baseline controller, i.e. is a disturbance to the NMPC, there remains an opportunity to review the baseline control strategy to not unnecessarily adjust this flow to compensate for density or level disturbances.

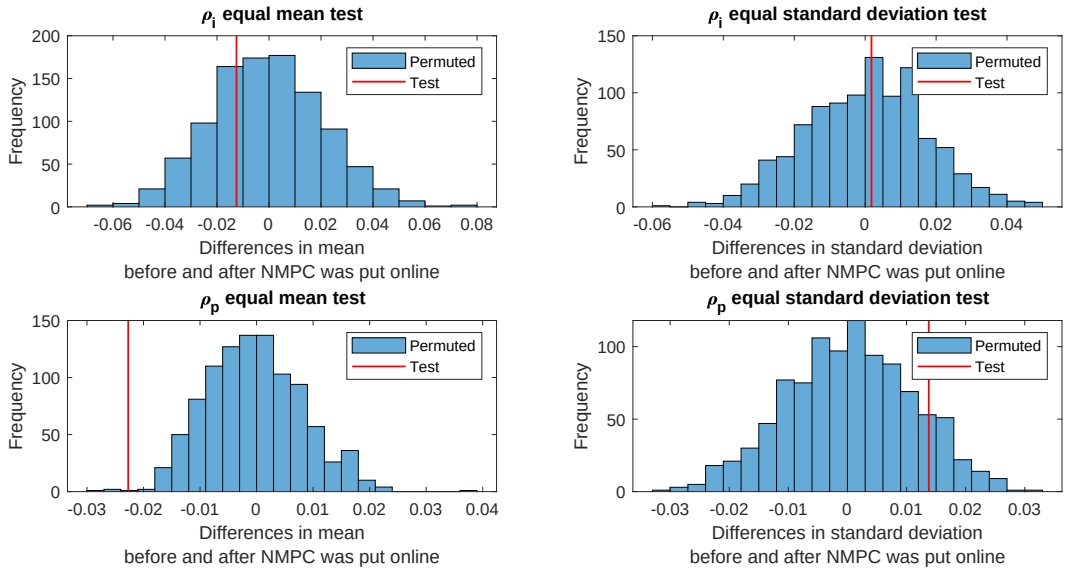

Figure 14: Permutation test results for the input (top row) and output (bottom row) densities of the plant, recorded before and after the NMPC was put online.

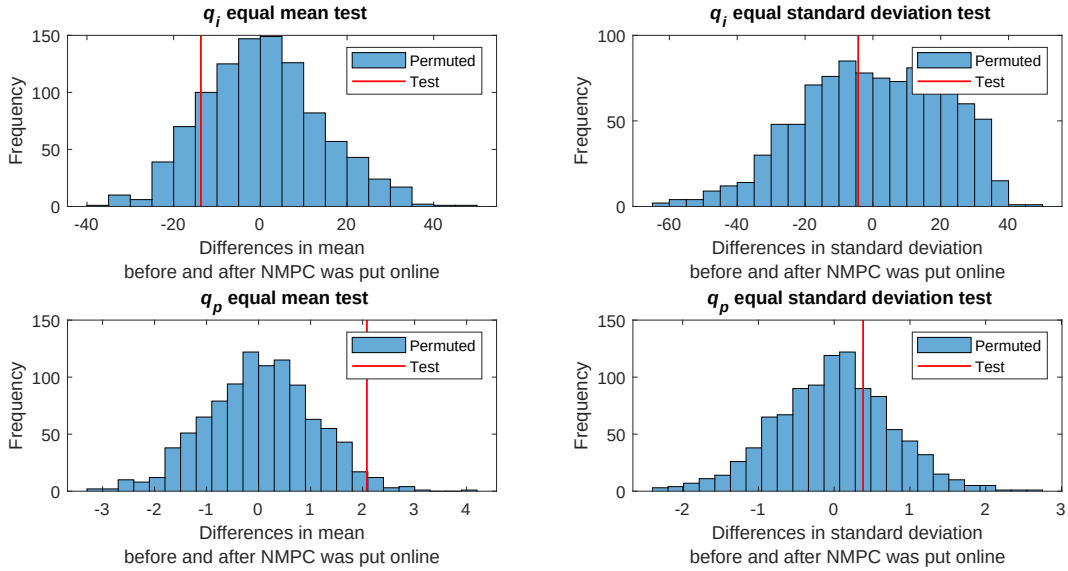

Figure 15: Permutation test results for the input (top row) and output (bottom row) flows of the plant, recorded before and after the NMPC was put online.

Table 4 presents a summary of the results using the permutation method for comparing two independent groups, as described in Wilcox (2003). For each key plant variable a permutation test was performed to determine if there is a statistically significant difference between its mean or standard deviation before and after the NMPC was put online. The null hypothesis h_0 of equal mean or equal standard deviation is rejected with 5 % confidence if the significance value is less than 0.05.

Figures 14 to 16 present the individual permutation tests from Table 4. For each test in these figures a positive test statistic (red) would indicate that the mean or standard deviation has decreased after the NMPC was put online. Alternatively, a negative test statistic would indicate that the mean or standard deviation has increased after the NMPC was put online.

Figure 14 and Table 4 show that both the mean and standard deviation of the input density to the plant ρ_i is comparable for the periods before and after the NMPC is put online. There is no significant difference in the standard deviation of plant output density ρ_p, however, the mean plant output density has significantly increased

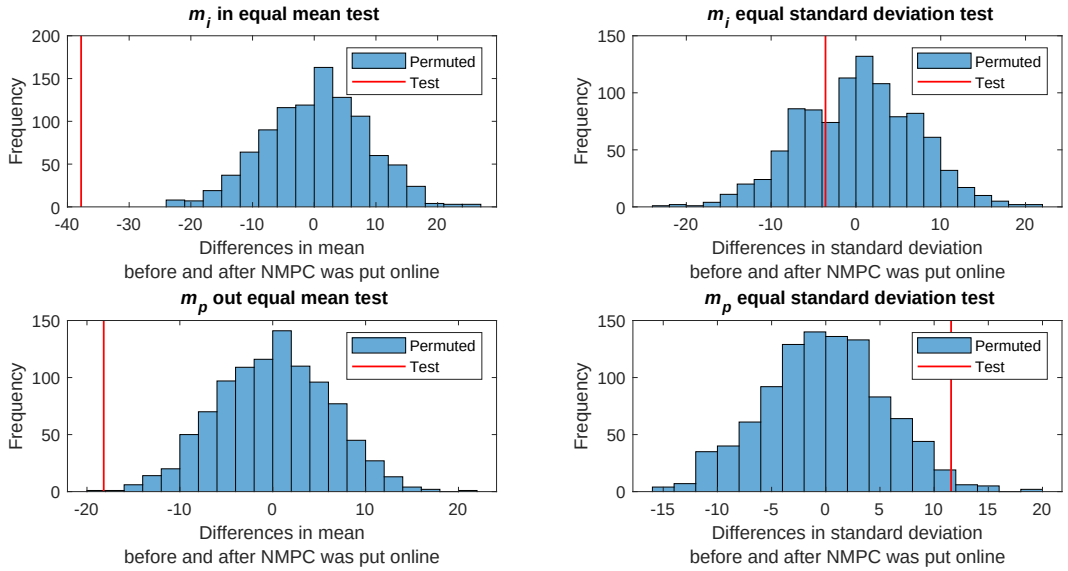

Figure 16: Permutation test results for the input (top row) and output (bottom row) mass flows of the plant, recorded before and after the NMPC was put online.

while the NMPC was online. A comparable mean plant input density with a significantly higher plant output density can only be explained by improved dewatering ability of the plant while the NMPC was online.

Figure 15 and Table 4 show that while there is no significant difference in the mean input flow to the plant q_i, the mean output flow from the plant q_p is significantly lower while the NMPC was online. This lower volumetric flow rate of tailings from the plant can also be explained by an increase in the dewatering ability of the plant with the NMPC online, considering that an increase in water recovered via the thickener overflow would imply less water reporting to the plant output.

The concentration of solids by weight in a slurry c_s is calculated as follows:

$$c_s = 100 \left(\frac{\frac{\rho_s}{\rho_{sl}} - \rho_s}{1 - \rho_s} \right), \tag{17}$$

with ρ_s the density of the solids and ρ_{sl} the density of the slurry. Plant operations assume a solids density of $\rho_s = 4.1$ t/m^3. By comparing the difference between the concentration of solids in the plant output before and after the NMPC is put online, it is possible to show that an additional 0.063 ton water was recovered for every ton solids produced when the NMPC was online. This amounts to approximately 13 m^3/h, or 5 % of the water contained in the tailings product of the plant.

Both the mean mass flow into and out of the plant, m_i and m_p, are significantly higher for the period when the NMPC was online, as shown in Figure 16 and Table 4. The standard deviation of the input mass flow was comparable, while the standard deviation for the output mass flow significantly lower while the NMPC was online. The variability of the mass flow from the plant is therefore improved, with a 27 % lower standard deviation, while the NMPC was online.

7. Conclusions

A nonlinear model predictive controller (NMPC) was implemented on the surge tank of an industrial tailings retreatment circuit. This controller was developed following a general control problem framework. First, a rigorous nonlinear model was derived for the surge tank from first principles, and validated using pure simulation. Then, a control design and analysis was performed motivating for an NMPC to be implemented on the plant. Finally the controller was implemented using non-proprietary software.

The results show that the variability of the mass flow of tailings from the plant was significantly reduced under NMPC control. The plant also delivered a higher output density, while there were no significant difference in the input density to the plant. Therefore, under NMPC control the plant showed improved dewatering ability.

References

Adetola, V., DeHaan, D., Guay, M., 2009. Adaptive model predictive control for constrained nonlinear systems. Systems and Control Letters 58 (5), 320–326.

Alcalde, J., Kelm, U., Vergara, D., 2018. Historical assessment of metal recovery potential from old mine tailings: A study case for porphyry copper tailings, Chile. Minerals Engineering 127, 334–338.

Bauer, M., Craig, I. K., 2008. Economic assessment of advanced process control - A survey and framework. Journal of Process Control 18 (1), 2–18.

Beal, L. D. R., Hill, D. C., Martin, R. A., Hedengren, J. D., 2018. Gekko optimization suite. Processes 6 (8).
URL http://www.mdpi.com/2227-9717/6/8/106

Blomsma, F., Brennan, G., 2017. The emergence of circular economy: A new framing around prolonging resource productivity. Journal of Industrial Ecology 21 (3), 603–614.

Craig, I. K., 1997. On the role of the general control problem in engineering education. IFAC Proceedings Volumes 30 (12), 201–204.

Craig, I. K., Henning, R. D. G., 2000. Evaluation of advanced industrial projects: A framework for determining economic benefit. Control Engineering Practice 8, 769–780.

Crisafulli, S., Peirce, R. D., 1999. Surge tank control in a cane raw sugar factory. Journal of Process Control 9, 33–39.

Dontsov, E. V., Perice, A. P., 2014. A new technique for proppant schedule design. Hydraulic Fracturing Journal 1 (3), 1–8.

Falagán, C., Grail, B. M., Johnson, D. B., 2017. New approaches for extracting and recovering metals from mine tailings. Minerals Engineering 106, 71–78.

Ghodrat, M., Qi, Z., Kuang, S. B., Ji, L., Yu, A. B., 2016. Computational investigation of the effect of particle density on the multiphase flows and performance of hydrocyclones. Minerals Engineering 90, 55–69.

Gros, S., Mario, Z., Rian, Q., Bemporad, A., Moritz, D., 2020. From linear to nonlinear MPC: Bridging the gap via the real-time iteration. International Journal of Control 93 (1), 62–80.

Ilka, A., Veseleý, V., 2015. Gain-scheduled MPC design for nonlinear systems with input constraints. IFAC-PapersOnLine 48 (11), 912–917.

Khan, K., Spurgeon, S., 2006. Robust MIMO water level control in interconnected twin-tanks using second order sliding mode control. Control Engineering Practice 14, 375–386.

Kossoff, D., Dubbin, W. E., Alfredson, M., Edwards, S. J., Macklin, M. G., Hudson-Edwards, K. A., 2014. Mine tailings dams: Characteristics, failure, environmental impacts, and remediation. Applied Geochemistry 51, 229–245.

Lambooy, T., 2011. Corporate social responsibility: Sustainable water use. Journal of Cleaner Production 19, 852–866.

Lee, M., Shin, J., 2009. Constrained optimal control of liquid level loops using a conventional proportional-integral controller. Chemical Engineering Communications 196, 729–745.

Luyben, W. L., 2020. Liquid level control: Simplicity and complexity. Journal of Process Control 86, 57–64.

Martin, T. E., McRoberts, E. C., 1999. Some considerations in the stability analysis of upstream tailings dams. In: Proceedings of the Sixth International Conference on Tailings and Mine Waste, Fort Collings, Colorado, USA, 24-27 January 1999. A.A Balkema Rotterdam, pp. 1–17.

Meyer, E. J., Olivier, M. C., Matumba, L., Craig, I. K., 2019. Model predictive control and simulation, implementation and performance assessment of a coal comminution circuit. Minerals Engineering 144, 1–14.

Murad, S. A., 2017. Environment, social, and governance (ESG) criteria and preferences of managers. Taylor & Francis, Abingdon.

Ntengwe, F., Witika, L. K., 2011. Optimization of the operating density and particle size distribution of the cyclone overflow to enhance the recovery of flotation of copper sulphide and oxide minerals. Journal of the South African Institute of Mining and Metallurgy 111 (4), 295–300.

Olivier, L. E., Craig, I. K., 2015. Development and application of a model-plant mismatch expression for linear time-invariant systems. Journal of Process Control 32, 77–86.

Qin, S. J., Badgwell, T. A., 2003. A survey of industrial model predictive control technology. Control Engineering Practice 11 (7), 733–764.

Reyes-Lúa, A., Backi, C. J., Skogestad, S., 2018. Improved PI control for a surge tank satisfying level constraints. IFAC-PapersOnLine 54 (4), 835–840.

Roche, C., Thygesen, K., Baker, E., 2017. Mine tailings storage: Safety is no accident. (A UNEP rapid response assessment. United Nations Environment Programme and GRID-Arendal).
URL www.grida.no (Accessed:19 May 2022)

Rokebrand, L. L., Burchell, J. J., Olivier, L. E., Craig, I. K., 2020. Competing advanced process control via an industrial automation cloud platform. ArXiv, arXiv:2011.13184.

Rokebrand, L. L., Burchell, J. J., Olivier, L. E., Craig, I. K., 2021. Towards an access economy model for industrial process control: A bulk tailings treatment plant case study. IFAC-PapersOnLine 54, 121–126.

Rosander, P., Isaksson, A. J., Löfberg, J., Forsman, K., 2012. Practical control of surge tanks suffering from frequent inlet flow upsets. IFAC Proceedings Volumes 45, 258–263.

Russell, A., 2020. Online spiral grade control. Journal of the Southern African Institute of Mining and Metallurgy 120, 113 – 119.

Sanchis, R., Romero, J. A., Martin, J. M., 2011. A new approach to averaging level control. Control Engineering Practice 19, 1037–1043.

Santamarina, J. C., Torres-Cruz, L. A., Bachus, R. C., 2019. Why coal ash and tailings dam disasters occur: Knowledge gaps and management shortcomings contribute to catastrophic dam failures. Science 364 (6440), 526–528.

Sbarbaro, D., Ortega, R., 2007. Averaging level control: An approach based on mass balance. Journal of Process Control 17, 621–629.

Skogestad, S., Postlethwaite, I., 2005. Multivariable Feedback Control: Analysis and Design, 2nd Edition. John Wiley and Sons.

Sparbaro, D., Ortega, R., 2007. Averaging level control: An approach based on mass balance. Journal of Process Control 17, 621 – 629.

Umadevi, T., Kumar, A., Umashanker, A., Sah, R., Marutiram, K., 2021. Performance evaluation of a laboratory floatex density separator and its comparison with a spiral concentrator. Mineral Processing and Extractive Metallurgy 130 (2), 118–125.

Wiid, A. J., le Roux, J. D., Craig, I. K., 2021. Pressure buffering control to reduce pollution and improve flow stability in industrial gas headers. Control Engineering Practice 115, 104904.

Wilcox, R., 2003. Applying Contemporary Statistical Techniques, 1st Edition. Elsevier.

Zeng, X., Tongxin, X., Guochang, X., Albalghiti, E., Shan, G., Li, J., 2021. Comparing the costs and benefits of virgin and urban mining. Journal of Management Science and Engineering 7 (1), 98–106.